A Multiterminal Setup for Complex Dynamics Characterization and Unconventional Computing in Self-Organizing Memristive Networks

A multiterminal setup for complex dynamics characterization and unconventional computing in self-organizing memristive networks

1st Davide Pilati
Department of Applied science and technology
Politecnico di Torino
C.so Duca degli Abruzzi 24, 10129
Torino, Italy
davide.pilati@polito.it

2nd Fabio Michieletti
Department of Applied science and technology
Politecnico di Torino
C.so Duca degli Abruzzi 24, 10129
Torino, Italy
fabio.michieletti@polito.it

3rd Alessandro Cultrera
Quantum metrology and nanotechnologies
INRiM, Istituto Nazionale di Ricerca Metrologica
Torino, 10135 Italy
a.cultrera@inrim.it

4th Carlo Ricciardi
Department of Applied science and technology
Politecnico di Torino
C.so Duca degli Abruzzi 24, 10129
Torino, Italy
carlo.ricciardi@polito.it

5h Gianluca Milano
Advanced metrology and Life Science division
INRiM, Istituto Nazionale di Ricerca Metrologica
Torino, 10135 Italy
g.milano@inrim.it

Abstract*—The recent growing interest in neuromorphic architectures based on emergent dynamics of self-organizing memristive networks has posed some challenges regarding the spatiotemporal characterization of these multiterminal systems. This work presents a versatile measurement platform specifically designed for the characterization of memristive nanowire networks and for testing the implementation of unconventional computing paradigms in these systems. By integrating an FPGA controlled, parallel multiterminal array of source-measure units with a custom fixture based on spring-loaded electrodes, the system allows for real-time, reconfigurable voltage and current measurements across 16 terminals without hardware reconnections. The platform supports seamless transition between conventional two-terminal characterization, multiterminal characterization and testing computational properties in the framework of physical reservoir computing. Local conductance measurements, voltage mapping, and real-time dynamic monitoring offer unique insights into the spatiotemporal behavior of the networks. Furthermore, we show that the system enables to correlate electrical properties of the multiterminal network in terms of conductance matrices and voltage maps with computational performances, allowing also adaptive control over the network's operating state. The here reported setup provides a versatile platform for computing at the matter level (i.e., in materia) with multiterminal systems based on self-organizing memristive networks.

Keywords — Self-organizing Memristive Networks, Multiterminal Characterization, Physical Reservoir Computing, Neuromorphic Computing, Spatiotemporal Dynamics

I. Introduction

The rapid advancements in machine learning and artificial intelligence have recently brought attention to unconventional computing architectures to improve energy efficiency. Neuromorphic systems have gained popularity as promising candidates to address these limitations, given their inherent similarity to biological neural networks [1]. Among them, self-organizing memristive networks made of nanoelements showed brain-like dynamics such as short/long term synaptic plasticity, criticality and emergent behavior [2], [3], [4], [5], [6]. These neuromorphic features have been exploited for unconventional computing paradigms such as Reservoir Computing (RC) [2], [7], [8], [9], [10]. In particular, the RC paradigm exploits the spatiotemporal dynamics of these systems to cast an input to a higher dimension feature space (the reservoir), relying on an external readout layer to perform the training. The reservoir is often modeled as a recurring neural network, but when physical systems act as reservoir, the paradigm is called physical reservoir computing (PRC) [11]. Using self-organizing, nonlinear dynamic systems as physical reservoir has been shown to be a promising hardware solution for a variety of tasks [7], [10], [12], [13], [14], [15]. However, understanding the relationship between dynamics of these systems and their computational capabilities still represents a challenge. Traditional two terminal measurements fall short in analyzing the complex spatiotemporal dynamics of self-organizing systems, where the emergent and spatially distributed nature of their behavior requires the development of multiterminal characterization techniques. Although multiterminal systems can capture spatiotemporal data, they often do so at the cost of measurement setup versatility. The most common characterization setup for these networks is composed of one or more waveform generators paired with a series of Analog-to-Digital Converters (ADC) that allow measuring physical observables over multiple points of the Device Under Test (DUT) area [14], [16]. In these conventional measurement systems, a switching matrix is employed to route bias signals to different DUT terminals, while in more rudimentary approaches, manual reconfiguration of the electrical connections may represent the only viable alternative. Moreover, sputtered electrodes are required to achieve electrical contact between the DUT and the measurement system.

In this work, we present a versatile platform that enables comprehensive investigation of the interplay between electrical and computational properties of self-organizing systems. This setup can provide up to 16 parallel Source-Measure Unit (SMU) channels, addressing the limitations of conventional methods. This setup can cover a variety of characterization routines as well as exploiting the DUT spatiotemporal dynamics in a PRC framework.

II. Measurement Setup

The measurement setup proposed in this work (Figure 1) is built around a fully parallel SMU array controlled by an FPGA-based system that features 64 independent channels capable of simultaneous voltage sourcing and current measurement (ArC TWO by ArC Instruments) [17]. This degree of parallelism minimizes the delay introduced by

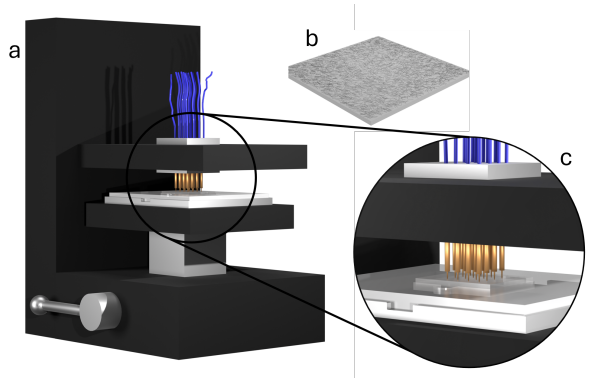

Figure 1. Multiterminal grid measurement setup. a) 4x4 grid fixture made of 16 pogo-pins in contact with the DUT. b) DUT, NW network, 1x1 cm quartz sample drop-casted with an Ag-PVP NW suspension. c) enhancement of a), the gold-plated pins are pushed on the sample to achieve electrical contact. The pressure exerted by the gold pins is sufficient to break the PVP coating of the NW and directly contact the Ag core.

traditional multichannel sequential measurements, allowing for real-time configuration switching during data acquisition. This measurement unit is complemented by a custom design fixture (Figure 1a) featuring a 4x4 grid of spring-loaded gold-plated pogo pins which ensures a reliable electrical contact between the measurement setup and the DUT (Figure 1b and c), eliminating the need for electrode bonding and, in some cases (as in this work), even removing the need for conventional lithographically defined contact pads, as shown in [18], [19], [20].

The proposed setup is an integrated platform that can implement a wide range of functionalities. It supports flexible routing since each channel can be independently biased, grounded or set to float, allowing a comprehensive understanding of conductance and voltage distribution across the network [9], [21]. This flexibility is what enables the system to seamlessly transition from characterization measurements to computing tasks, without reconfiguring hardware contacts.

The above-described measurement setup is programmed with a custom-developed Python code that can perform pre-defined characterization routines or adapt in real-time based on the acquired data. The measurements reported in this work are collected on multiterminal Ag-PVP nanowire (NW) networks, a self-organizing system that has been shown to endow memristive dynamics [6].

III. Results and Discussion

Here follows an overview of a measurement routine that features both characterization and implementation of computing tasks.

A. Pristine State Evaluation

The first measurement is devoted to identifying the pristine conductive state of a multiterminal self-organizing network. Bias and ground are set at opposing sample corners and the conductance $G_{1,16}$ (see Figure 2a) is determined by applying a reading voltage (maximum 0.01 V in magnitude). The current is read at the same contacts to determine whether the sample (seen from these electrodes) is already conducting without any forced electrical activation. Since we want to control the operational state of the network during computing operation, depending on the pristine state, we may decide to apply a voltage ramp or a constant voltage to furtherly increase the conductance, or simply reject the sample because of a too high conductive state. In case of a low conductive sample, a python algorithm can be exploited to automatically switch to an activation protocol (typically a voltage ramp on the same bias electrode used for measuring the pristine state) that can automatically stop at the desired conductance level thanks to real-time data analysis.

B. Conductance Matrix

Once the sample is brought to the desired operational state, the system enables to characterize the conductance locally, between all contact pairs in a sequential manner. First $G_{1,2}$ is measured by applying a reading voltage to electrode 1, imposing 0 V to electrode 2, and reading the current (Figure 2a). $G_{1,2}$ is therefore obtained as

$$G_{1,2} = \frac{I_{1,2}}{V_{1,2}}$$

This process is repeated sequentially for all the possible pairs that require the bias to be imposed to electrode 1 ($G_{1,3}$, $G_{1,4}$, and so on). Then the voltage bias is moved to electrode 2 and since $G_{1,2}$ has already been evaluated, the combinations start

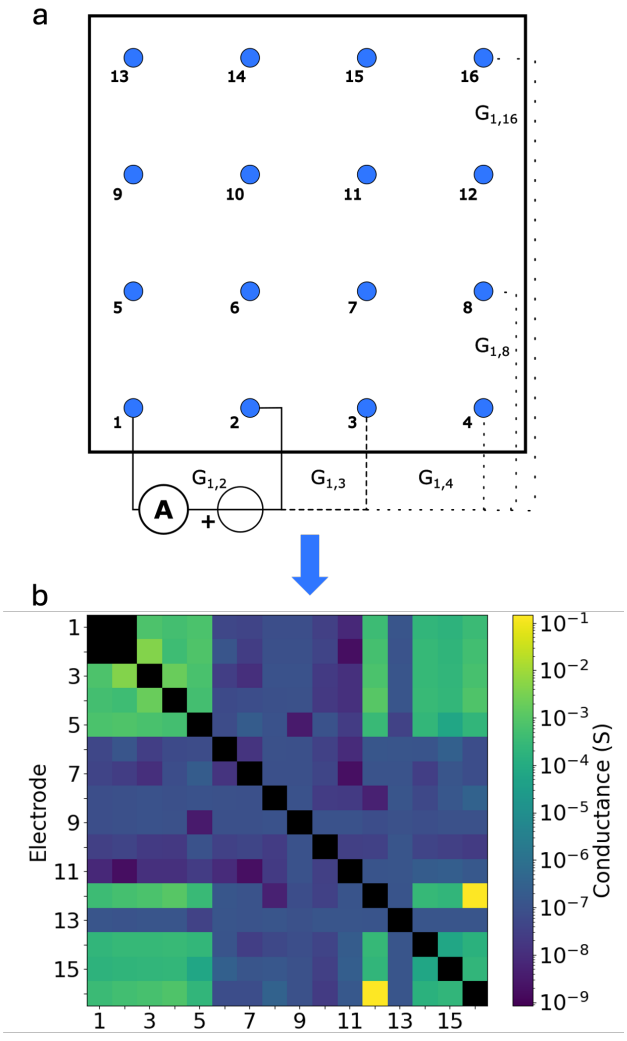

Figure 2. Conductance matrix measurement protocol. a) Each electrode pair conductance is measured by applying a voltage and reading the current. This process is repeated until all the electrode combinations have been tested, to obtain b) the conductance matrix.

with $G_{2,3}$ and end with $G_{2,16}$. All electrode combinations are covered in this way up to the last measurement, which is $G_{15,16}$. The conductance matrix M is filled in its upper triangular part with the conductance measurements so that the conductance $G_{i,j}$ is placed in $M_{i,j}$ (Figure 2b). For visualization purposes the matrix is then mirrored on its diagonal.

This routine is a two-terminal procedure that in a traditional setup would require a switching matrix to reconfigure bias and ground on the desired contact pairs. Thanks to the independent configuration capabilities of the here reported setup, a switching matrix is not needed, and the whole measurement routine is therefore completed faster. The time required for completing such routine for a 16 terminal setup is reduced from ~135s (similar procedure, switching matrix-based setup described in [18]) to ~2s (this work).

C. Voltage Maps

It is to be underlined that all the previously described characterizations are based on traditional two-terminal measurements, but thanks to the parallel nature of the setup, voltage can be monitored simultaneously on all 16 contacts while performing both pristine state evaluation and activation protocols just by setting the remaining 14 channels to float (Figure 3a). The simultaneous voltage sampling across the network in response to an applied input voltage allows the reconstruction of a voltage map (Figure 3b), i.e. a snapshot of the spatial voltage distribution on the DUT area.

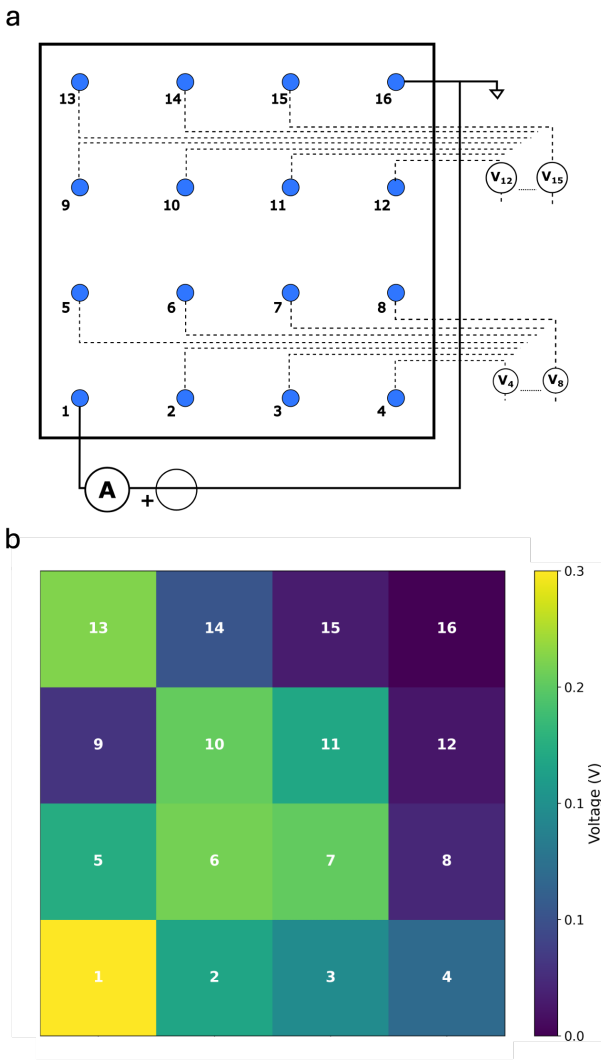

Figure 3. Schematics of a reservoir computing application. a) Voltage bias is applied to electrode 1, electrode 16 is set to ground and the voltage is measured in a floating way on all the other 14 electrodes. b) Voltage map of a MC measurement at t = 300 s, representing the spatialization of the instantaneous voltage distribution as a response to the input. Each floating electrode is treated as a node for a reservoir computing application.

D. Conductance Matrices vs Voltage Maps

The information obtained through voltage maps is fundamentally different with respect to the one obtained with a conductance matrix. The voltage distribution is a direct consequence of the internal rearrangements of the reservoir in response to an electrical stimulus. However, differently from conductance matrices, the representation obtained by voltage maps is dependent on the bias choice both in terms of magnitude and spatial location (i.e. the voltage map with bias on electrode 1 will be different with respect to the voltage map with bias on electrode 2). In a conductance matrix instead, the reading source is constantly moving and the information gained is about the local conductance seen by the two terminals involved. It turn out that if for some reason the chosen bias electrode is isolated from the rest of the network (there isn't a NW path connecting the bias electrode with the rest of the network), a voltage map does not provide any information, while a conductance matrix can still show how the rest of the network is connected. Nevertheless, being able to simultaneously measure voltage on all channels opens for computing applications where accessing the system simultaneously through different electrodes is crucial for exploiting the DUT as a reservoir in a PRC framework. In this context, voltage readings represent the best choice to simultaneously access the internal state of the system in different spatial location.

E. Implementation of computing tasks

In order to exploit these devices for computing purposes, one or more input signals have to be fed to one or more input electrodes, a reference voltage (usually 0 V) has to be fixed to one or more electrodes, and the rest of the electrodes must act as floating voltage probes to extract reservoir outputs (i.e. voltage maps and their evolution over time)that are used for computing purposes. The measurement setup described in this work can provide arbitrary waveforms to each terminal independently, allowing for multiple simultaneous inputs that can rearrange on the network over time if needed, while probing floating voltage on an arbitrary number of other electrodes. In this work we report as an example the implementation of the Memory Capacity (MC) task, which is a common benchmark in reservoir computing frameworks [22], [23], [24]. In this task, one electrode is set to ground, and 14 voltage outputs are read from the network simultaneously. Having SMUs instead of conventional waveform generators and ADC allows to directly measure the current of the ground and bias terminals (without relying on indirect measurements on external load resistors), which gives information about the system conductance state during the task. Having this kind of information is crucial to determine if the network can withstand further stimuli without excessive potentiation or if the routine needs to be paused to allow network relaxation. The measurement system gives real-time data to the controller PC; therefore, the programmed routine can perform these checks autonomously. A random input $v(t)$ with uniform distribution in a voltage range is applied to the network.

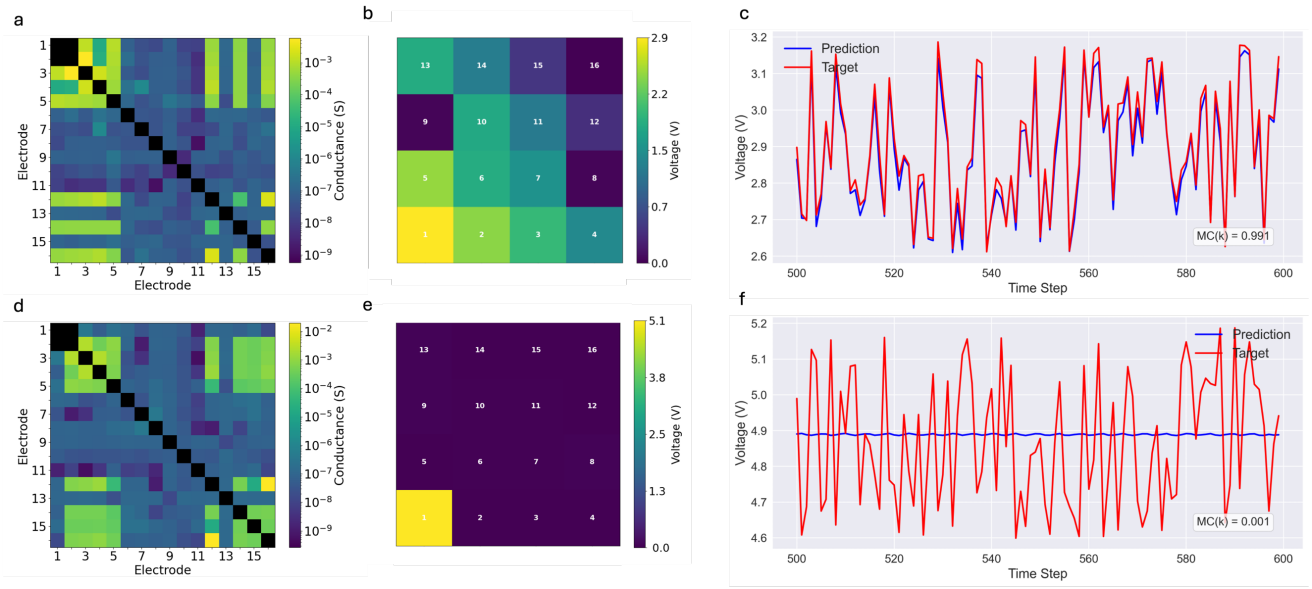

Figure 4. MC as a function of the measurement number. A series of MC evaluations has been conducted over time, while the conductance state of the DUT was evaluated by conductance matrix analysis in between MC measurements. The reported results refer to two different reservoir states: state 1 (a, b, c), and state 2 (d, e, f). a) Conductance matrix of the sample in reservoir state 1. b) Voltage map during MC routine, timestep 1500 (t = 300 s), reservoir state 1. c) MC target and predicted waveform for delay k = 1, reservoir state 1. d) Conductance matrix of the sample in reservoir state 2. e) Voltage map during MC routine, timestep 1500 (t = 300 s), reservoir state 2. c) MC target and predicted waveform for delay k = 1, reservoir state 2.

$$v(t) \sim U([V_{min}, V_{max}])$$

The output nodes voltages are measured at each timestep, providing a picture of the reservoir state and of its evolution over time. These voltages are fed to a regression layer which is trained to reconstruct a delayed version of the input waveform. The goal is to reconstruct a series of delayed inputs for a range of k delays. The MC is evaluated for each k as

$$\mathrm{MC}_k = \frac{\mathrm{cov}^2\left(v(t-k), y_k(t)\right)}{\sigma^2\left(v(t)\right)\sigma^2\left(y_k(t)\right)}$$

where y_k is the target waveform for delay k. The total value of MC is then computed as

$$\mathrm{MC} = \sum_{k=1}^{\infty} \mathrm{MC}_k$$

The network is first characterized by means of a conductance matrix (Figure 4a, d), followed by the evaluation of the MC. Figure 4 reports two different operational states to which the reservoir has been programmed. For clarity we are going to call these two states "reservoir state 1" (Figure 4a, b, c) and "reservoir state 2" (Figure 4d, e, f). When the DUT is in the reservoir state 1, the instantaneous voltage maps (obtained by applying a bias of 2.9 V in between electrodes 1 and 16) look like the one reported in Figure 4b, with a voltage distribution that covers the majority of the electrodes. This translates in a global involvement of the reservoir in computing operations, and in a successful reconstruction of the target for a delay k = 1 (Figure 4c, MC_k = 0.991). The operational state 2 is instead identified by a break in the NW connections between the bias electrode and the rest of the network. This can be seen in the conductance matrix as reported in Figure 4d, as the row relative to electrode 1 shows that all its connections with other electrodes have extremely low conductance. Furthermore, the voltage map reported in Figure 4e confirms this, as the bias imposed to electrode 1 is not able to reach any other part of the DUT (due to the extremely low conductance between the bias electrode and the rest of the network). Indeed, in this particular case, the voltage map does not provide any useful information regarding the internal reservoir state. This results in a drop of MC and the inability to reconstruct any waveform (Figure 4f, MC_k = 0.001). Thanks to the conductance matrix analysis, though, we are still able to monitor the internal reservoir state. As demonstrated by the matrix reported in Figure 4d, the matrix pattern has changed with respect to the operational State 1 (Figure 4a), opening the possibility for studying other bias configurations to exploit a network that would otherwise be considered not suitable for computing applications.

IV. Conclusions

In summary, the proposed measurement setup offers a versatile platform for probing the complex dynamics of neuromorphic networks for unconventional computing. By combining a fully parallel and reconfigurable SMU system with a custom multiterminal fixture, the proposed platform is capable of real-time spatiotemporal monitoring of complex network dynamics. The approach used allows for a comprehensive monitoring of the conductive state of the system both on a global and a local level enabling the possibility of managing the operating conditions of the network by tuning the network states through local stimulations. Furthermore, this system can be used for the implementation of various PRC routines and for experimental implementation of computing tasks which have been tested in simulations [5], [25], [26], [27]. By demonstrating a correlation between the internal state of the system in terms of conductance matrices/voltage maps and computing performance, this work highlights the importance of monitoring the reservoir state during computational routines.

The high-throughput, parallel measurement capability, combined with the flexible electrode configuration and easy contacting procedure enabled by the custom pogo pin fixture, provides a solution for harnessing spatiotemporal dynamics in self-organizing nanoscale networks.

ACKNOWLEDGMENT

The authors would like to thank Mr. Danilo Serazio (INRiM) for the fabrication and design of the custom-made fixture. Part of this work has been supported by funding by NEURONE, a project funded by the European Union - Next Generation EU, M4C1 CUP I53D23003600006, under program PRIN 2022 (prj code 20229JRTZA). Part of this work has been supported by the European Research Council (ERC) under the European Union's ERC Starting Grant (ERC-2024-STG) agreement "MEMBRAIN" No. 101160604.

REFERENCES

[1] D. V Christensen *et al.*, '2022 roadmap on neuromorphic computing and engineering', *Neuromorphic Computing and Engineering*, vol. 2, no. 2, p. 022501, Jun. 2022, doi: 10.1088/2634-4386/ac4a83.

[2] A. Z. Stieg, A. V Avizienis, H. O. Sillin, C. Martin-Olmos, M. Aono, and J. K. Gimzewski, 'Emergent Criticality in Complex Turing B-Type Atomic Switch Networks', *Advanced Materials*, vol. 24, no. 2, pp. 286–293, Jan. 2012, doi: 10.1002/adma.201103053.

[3] G. Milano, E. Miranda, and C. Ricciardi, 'Connectome of memristive nanowire networks through graph theory', *Neural Networks*, vol. 150, pp. 137–148, Jun. 2022, doi: 10.1016/J.NEUNET.2022.02.022.

[4] A. Diaz-Alvarez *et al.*, 'Emergent dynamics of neuromorphic nanowire networks', *Sci Rep*, vol. 9, no. 1, Oct. 2019, doi: 10.1038/s41598-019-51330-6.

[5] G. Milano, F. Michieletti, D. Pilati, C. Ricciardi, and E. Miranda, 'Self-organizing neuromorphic nanowire networks as stochastic dynamical systems', *Nat Commun*, vol. 16, no. 1, p. 3509, Apr. 2025, doi: 10.1038/s41467-025-58741-2.

[6] G. Milano *et al.*, 'Brain-Inspired Structural Plasticity through Reweighting and Rewiring in Multi-Terminal Self-Organizing Memristive Nanowire Networks', *Advanced Intelligent Systems*, vol. 2, no. 8, p. 2000096, Jan. 2020, doi: 10.1002/AISY.202000096.

[7] A. Loeffler *et al.*, 'Neuromorphic learning, working memory, and metaplasticity in nanowire networks', *Sci Adv*, vol. 9, no. 16, Apr. 2023, doi: 10.1126/sciadv.adg3289.

[8] R. K. Daniels, J. B. Mallinson, Z. E. Heywood, P. J. Bones, M. D. Arnold, and S. A. Brown, 'Reservoir computing with 3D nanowire networks', *Neural Networks*, vol. 154, pp. 122–130, Oct. 2022, doi: 10.1016/j.neunet.2022.07.001.

[9] F. Michieletti, D. Pilati, G. Milano, and C. Ricciardi, 'Self-organized Criticality in Neuromorphic Nanowire Networks With Tunable and Local Dynamics', *Adv Funct Mater*, Mar. 2025, doi: 10.1002/adfm.202423903.

[10] G. Milano *et al.*, 'In materia reservoir computing with a fully memristive architecture based on self-organizing nanowire networks', *Nat Mater*, vol. 21, no. 2, pp. 195–202, Oct. 2021, doi: 10.1038/s41563-021-01099-9.

[11] K. Nakajima, 'Physical reservoir computing—an introductory perspective', *Jpn. J. Appl. Phys. (2008)*, vol. 59, no. 6, p. 60501, Jun. 2020.

[12] G. Tanaka *et al.*, 'Recent advances in physical reservoir computing: A review', *Neural Networks*, vol. 115, pp. 100–123, Jul. 2019, doi: 10.1016/J.NEUNET.2019.03.005.

[13] R. Zhu *et al.*, 'Online dynamical learning and sequence memory with neuromorphic nanowire networks', *Nat Commun*, vol. 14, no. 1, p. 6697, Nov. 2023, doi: 10.1038/s41467-023-42470-5.

[14] J. B. Mallinson, J. K. Steel, Z. E. Heywood, S. J. Studholme, P. J. Bones, and S. A. Brown, 'Experimental Demonstration of Reservoir Computing with Self-Assembled Percolating Networks of Nanoparticles', *Advanced Materials*, Apr. 2024, doi: 10.1002/ADMA.202402319.

[15] Z. E Heywood, J. B Mallinson, P. J Bones, and S. A Brown, 'From "follow the leader" to autonomous swarming: physical reservoir computing in two dimensions', *Neuromorphic Computing and Engineering*, vol. 4, no. 3, p. 034011, Sep. 2024, doi: 10.1088/2634-4386/ad7314.

[16] J. Hochstetter, R. Zhu, A. Loeffler, A. Diaz-Alvarez, T. Nakayama, and Z. Kuncic, 'Avalanches and edge-of-chaos learning in neuromorphic nanowire networks', *Nature Communications 2021 12:1*, vol. 12, no. 1, pp. 1–13, Jun. 2021, doi: 10.1038/s41467-021-24260-z.

[17] P. Foster, J. Huang, A. Serb, S. Stathopoulos, C. Papavassiliou, and T. Prodromakis, 'An FPGA-based system for generalised electron devices testing', *Sci Rep*, vol. 12, no. 1, Dec. 2022, doi: 10.1038/S41598-022-18100-3.

[18] A. Cultrera, G. Milano, N. De Leo, C. Ricciardi, L. Boarino, and L. Callegaro, 'Recommended implementation of electrical resistance tomography for conductivity mapping of metallic nanowire networks using voltage excitation', *Sci Rep*, vol. 11, no. 1, p. 13167, Jun. 2021, doi: 10.1038/s41598-021-92208-w.

[19] G. Milano, A. Cultrera, L. Boarino, L. Callegaro, and C. Ricciardi, 'Tomography of memory engrams in self-organizing nanowire connectomes', *Nat Commun*, vol. 14, no. 1, p. 5723, Sep. 2023, doi: 10.1038/s41467-023-40939-x.

[20] G. Milano *et al.*, 'Mapping Time-Dependent Conductivity of Metallic Nanowire Networks by Electrical Resistance Tomography toward Transparent Conductive Materials', *Cite This: ACS Appl. Nano Mater*, vol. 2020, pp. 11987–11997, 2020, doi: 10.1021/acsanm.0c02204.

[21] D. Pilati, F. Michieletti, A. Cultrera, C. Ricciardi, and G. Milano, 'Emerging Spatiotemporal Dynamics in

Multiterminal Neuromorphic Nanowire Networks Through Conductance Matrices and Voltage Maps', *Adv Electron Mater*, vol. 10, no. 12, Dec. 2024, doi: 10.1002/aelm.202400750.

[22] H. Jaeger, 'Short term memory in echo state networks', *Technical Report 152, GMD*, 2002.

[23] A. Rodan and P. Tiňo, 'Simple Deterministically Constructed Recurrent Neural Networks', 2010, pp. 267–274. doi: 10.1007/978-3-642-15381-5_33.

[24] M. C. Soriano *et al.*, 'Delay-Based Reservoir Computing: Noise Effects in a Combined Analog and Digital Implementation', *IEEE Trans Neural Netw Learn Syst*, vol. 26, no. 2, pp. 388–393, Feb. 2015, doi: 10.1109/TNNLS.2014.2311855.

[25] G. Milano, K. Montano, and C. Ricciardi, 'In materia implementation strategies of physical reservoir computing with memristive nanonetworks', *J Phys D Appl Phys*, vol. 56, no. 8, Jan. 2023, doi: 10.1088/1361-6463/ACB7FF.

[26] G. Milano, T. Chakrabarty, and C. Ricciardi, 'Mackey-Glass Time Series Forecasting by Nanowire Networks', in *2023 IEEE International Conference on Metrology for eXtended Reality, Artificial Intelligence and Neural Engineering (MetroXRAINE)*, IEEE, Oct. 2023, pp. 989–994. doi: 10.1109/MetroXRAINE58569.2023.10405786.

[27] G. Milano, M. Agliuzza, N. de Leo, and C. Ricciardi, 'Speech recognition through physical reservoir computing with neuromorphic nanowire networks', in *2022 International Joint Conference on Neural Networks (IJCNN)*, IEEE, Jul. 2022, pp. 1–6. doi: 10.1109/IJCNN55064.2022.9892078.